Transport activity–dependent intracellular sorting of the yeast general amino acid permease

Natalie E. Cain and Chris A. Kaiser
Department of Biology, Massachusetts Institute of Technology, Cambridge, MA 02139

ABSTRACT Intracellular trafficking of the general amino acid permease, Gap1p, of *Saccharomyces cerevisiae* is regulated by amino acid abundance. When amino acids are scarce Gap1p is sorted to the plasma membrane, whereas when amino acids are abundant Gap1p is sorted from the *trans*-Golgi through the multivesicular endosome (MVE) and to the vacuole. Here we test the hypothesis that Gap1p itself is the sensor of amino acid abundance by examining the trafficking of Gap1p mutants with altered substrate specificity and transport activity. We show that trafficking of mutant Gap1p^{A297V}, which does not transport basic amino acids, is also not regulated by these amino acids. Furthermore, we have identified a catalytically inactive mutant that does not respond to complex amino acid mixtures and constitutively sorts Gap1p to the plasma membrane. Previously we showed that amino acids govern the propensity of Gap1p to recycle from the MVE to the plasma membrane. Here we propose that in the presence of substrate the steady-state conformation of Gap1p shifts to a state that is unable to be recycled from the MVE. These results indicate a parsimonious regulatory mechanism by which Gap1p senses its transport substrates to set an appropriate level of transporter activity at the cell surface.

INTRODUCTION

The yeast *Saccharomyces cerevisiae* encodes 24 members of the amino acid—polyamine–organocation (APC) superfamily of transporter proteins, which are responsible for transport of amino acids and other amines across the plasma membrane (Nelissen *et al.*, 1997; Jack *et al.*, 2000). APC proteins share a common topology with 12 *trans*-membrane domains (TMDs) and cytosolic N and C termini. The physiological function of individual APC family members can be deduced from their mode of regulation. For example, the activity of several transporters, including *AGP1*, *BAP2*, *BAP3*, *GNP1*, *TAT1*, and *TAT2*, has been shown to be induced by amino acids through regulation of the Ssy1p-Ptr3p-Ssy5p (SPS) amino acid

sensor complex (Didion *et al.*, 1998; Iraqui *et al.*, 1999; Forsberg *et al.*, 2001). Because the transporters regulated by the SPS complex have relatively low capacity and are most active when amino acids are present in the growth medium, these transporters are thought to function opportunistically to transport specific amino acids for use in protein synthesis. By contrast, Gap1p is a high capacity transporter of all naturally occurring amino acids as well as many amino acid analogues, and is inactive when amino acids are present in the growth medium (Grenson *et al.*, 1970; Chen and Kaiser, 2002). Gap1p is therefore thought to function as a high capacity scavenger of amino acids for use as a source of nitrogen.

Much of the change in Gap1p activity in response to amino acid abundance is due to regulated alternative trafficking patterns of Gap1p in the secretory pathway. At the *trans*-Golgi, Gap1p can proceed directly to the plasma membrane, or it can be directly sorted to the multivesicular endosome (MVE), ultimately to be delivered to the vacuole via the vacuolar protein-sorting pathway (Roberg *et al.*, 1997; Rubio-Texeira and Kaiser, 2006). Sorting to the MVE requires polyubiquitination on lysine 9 and/or 16 of Gap1p by the E3 ubiquitin ligase complex of Bul1p, Bul2p, and Rsp5p (Helliwell *et al.*, 2001; Soetens *et al.*, 2001). Deletion of the redundant *BUL1* and *BUL2* accessory proteins or mutation of both ubiquitin-acceptor lysines on Gap1p prevents ubiquitination of Gap1p and results in constitutive sorting of Gap1p to the plasma membrane. Such mutants that constitutively express Gap1p at the cell surface become

hypersensitive to amino acid analogues as well as to naturally occurring amino acids, probably because of aminoacyl tRNA mischarging brought about by imbalances in the intracellular concentration of amino acids (Risinger et al., 2006). We have used amino acid sensitivity to develop genetic screens for *GAP1* mutants that are resistant to some amino acids but remain sensitive to others as a means to find substrate selectivity mutants (Risinger et al., 2006).

In the absence of amino acids, such as in growth on ammonia as a nitrogen source, Gap1p that has been ubiquitinated and sorted to the MVE will recycle from the MVE to the plasma membrane, where it is active for uptake of extracellular amino acids (Roberg et al., 1997; Rubio-Texeira and Kaiser, 2006). In the presence of amino acids, this recycling of Gap1p from the MVE is blocked, and Gap1p is efficiently sorted to the vacuole. We have tested a variety of compounds for their ability to cause Gap1p sorting to the vacuole and have found that all naturally occurring amino acids (as well as amino acid analogues that carry both α-carboxylate and α-amino moieties) are effective at signaling for Gap1p sorting, regardless of their quality as a source of nitrogen (Chen and Kaiser, 2002). Moreover, mutants that cause overproduction of intercellular amino acids such as *mks1Δ* and temperature-sensitive alleles of *LST8*, which encode a subunit of the TORC1 complex, will also trigger Gap1p trafficking to the vacuole, despite the induction of many cellular responses associated with nitrogen starvation (Chen and Kaiser, 2002, 2003). Although the mechanism by which Gap1p recycling from the MVE to the plasma membrane is inhibited by amino acids is not understood, these pharmacological and genetic tests for the conditions required for sorting of Gap1p to the vacuole suggest that the sensor for amino acid signaling is not related to nitrogen availability but instead depends on direct recognition of the presence of amino acids themselves.

Because the broad spectrum of amino acids that are transport substrates for Gap1p largely coincides with the spectrum of compounds that can trigger Gap1p sorting to the vacuole, we suspected that Gap1p itself might be the sensor for amino acids. Furthermore, characterization of the nonubiquitinatable Gap1p^{K9R,K16R} allele revealed that complex mixtures of amino acids, such as casamino acids (CAS), that are not toxic to cells, will reversibly inactivate Gap1p^{K9R,K16R} transport activity as the protein remains at the cell surface. Importantly, a mutant of Gap1p, which has a selective defect for transport of arginine, is not inactivated at the cell surface by arginine (Risinger et al., 2006). These findings establish a precedent for Gap1p transport activity acting as a sensor of amino acids, in this case to reversibly regulate transporter activity itself.

In this article we apply a similar strategy using Gap1p mutants with altered specificity or transport activity to test the hypothesis that the sorting of Gap1p acts in an autoregulatory fashion, in which active turnover of amino acid substrates in the transport cycle prevents recycling to the plasma membrane and leads to Gap1p sorting to the vacuole.

RESULTS

Gap1p^{A297V} is defective for transport of basic amino acids

We previously isolated Gap1p^{A297V} as a substrate specificity mutant that did not transport citrulline or arginine, but was able to transport glycine (Risinger et al., 2006). We tested Gap1p^{A297V} for uptake of alanine, phenylalanine, threonine, glutamate, and lysine to further characterize its catalytic defect. A strain expressing *GAP1^{A297V}* showed the same impairment of transport of citrulline, arginine, and lysine as a *gap1Δ* strain (Figure 1A). Gap1p^{A297V} allowed normal transport of all other amino acids tested, although uptake of phenylalanine was decreased to approximately 50% of uptake observed

for wild-type Gap1p. Thus the transport defect for Gap1p^{A297V} appeared largely to affect amino acids with basic side chains. Notably, either cells containing Gap1p^{A297V} or *gap1Δ* cells were nevertheless able to transport significant amounts of lysine and arginine. Transport assays in *can1Δ* (Risinger et al., 2006) and *lyp1Δ* cells (unpublished data) showed that this residual transport activity was due to the activities of the basic amino acid permease (Can1p) and the lysine-specific permease (Lyp1p).

The Ala-297 residue, mutated in Gap1p^{A297V}, lies in the middle of TMD6 and thus could alter the amino acid binding pocket so as to exclude binding of basic residues. To test for a possible defect in binding of basic amino acids, we tested whether citrulline could act as a competitive inhibitor of glycine transport for Gap1p^{A297V}. Competition assays used either *GAP1^{K9R,K16R}* or *GAP1^{K9R,K16R,A297V}* expressed in a *gap1Δ can1Δ* strain, which allowed for maximum levels of the Gap1p at the plasma membrane. We first calculated the apparent K_m of glycine transport and found that Gap1p^{K9R,K16R} and Gap1p^{K9R,K16R,A297V} have similar K_m values for glycine: 20.0 ± 5.3 μM and 12.7 ± 1.12 μM, respectively (Figure 1B). Although there appeared to be an approximately twofold difference between the V_{max} for glycine uptake for Gap1p^{K9R,K16R} and Gap1p^{K9R,K16R,A297V} (1587 and 850.7 pmol/min, respectively), this difference is probably not due to a significant difference in the specific activity, but can most easily be explained by differences in the abundance of Gap1p at the plasma membrane in the two strains. We then tested the ability of unlabeled citrulline to act as a competitor for uptake of [^{14}C]-glycine. Citrulline could inhibit glycine uptake through both Gap1p^{K9R,K16R} and Gap1p^{K9R,K16R,A297V} (Figure 1, C and D). Using the Cheng–Prusoff equation (Cheng and Prusoff, 1973), we calculated K_I values for citrulline inhibition to be ~36.6 μM for Gap1p^{K9R,K16R} and ~35.6 μM for Gap1p^{K9R,K16R,A297V}. In parallel experiments using arginine as an inhibitor, we found that the K_I for arginine inhibition of [^{14}C]-glycine transport by Gap1p^{K9R,K16R,A297V} was the same as for Gap1p^{K9R,K16R} (unpublished data). Based on the ability of basic amino acids to compete for transport of glycine, basic amino acids appear to bind to the active site of Gap1p^{A297V} with the same affinity as for wild-type Gap1p. Thus we conclude that the Gap1p^{A297V} is blocked at a step of the transport cycle that takes place after binding of a basic amino acid. Perhaps Gap1p^{A297V} cannot undergo the conformational changes necessary to complete a transport cycle when a basic amino acid occupies the active site.

Previously we showed that reversible inactivation of intrinsic Gap1p activity at the cell surface requires active transport through Gap1p (Risinger et al., 2006). We therefore tested various amino acids and combinations of amino acids for their ability to inactivate Gap1p^{K9R,K16R,A297V} at the cell surface (Figure 2). Cells expressing Gap1p^{K9R,K16R,A297V} were cultured in either a basic amino acid mix (hereafter referred to as BAM) consisting of arginine, citrulline, and lysine at 1 mM each, and CAS, a mixture containing all amino acids except tryptophan, at 0.25% (approximately 10 mM total amino acid concentration). As expected, Gap1p^{K9R,K16R,A297V} was not inactivated by BAM (Figure 2A), but was inactivated by CAS to the same degree as Gap1p^{K9R,K16R} (Figure 2B). The failure of Gap1p^{K9R,K16R,A297V} to be inactivated at the cell surface by basic amino acids provides independent evidence that the Ala-297 to Val mutation specifically blocks completion of a transport cycle for basic amino acid substrates.

Sorting of Gap1p into the MVE requires direct recognition of transport substrates

Amino acid regulation of the distribution of Gap1p between the plasma membrane and the vacuole is primarily determined by the
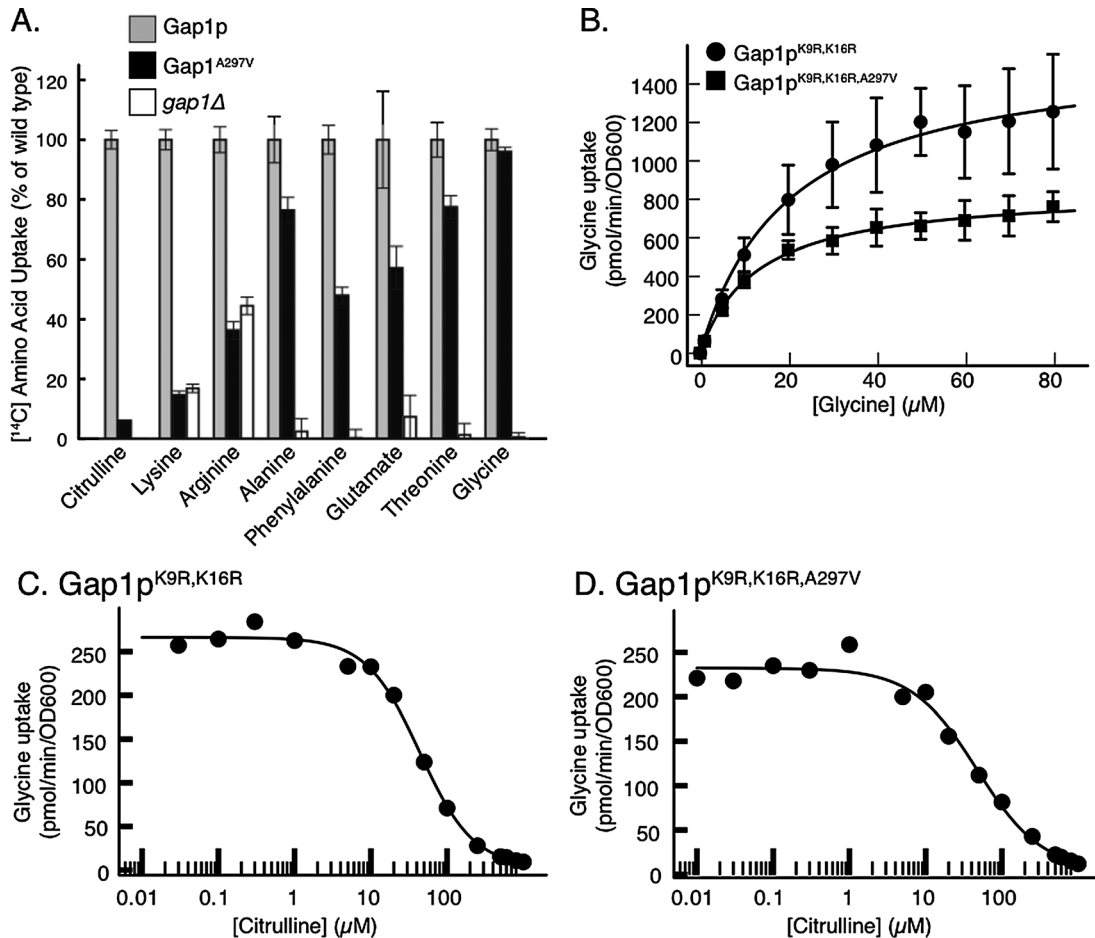
FIGURE 1: The Gap1p[A297V] mutant has a specific defect in transport of positively charged amino acids. (A) Initial rate of uptake for [14C]-labeled amino acids was determined for wild-type *GAP1* (pEC221), *gap1*[A297V] (pNC7), or empty vector (pRS316), expressed in a *gap1Δ bul1Δ bul2Δ* (CKY701) strain grown in SD medium. Mean uptake rates (n = 3) were normalized to the wild-type rate for each amino acid. (B) Kinetic parameters for [14C]-glycine uptake were determined for *gap1Δ can1* strains expressing P_{ADH1}-*GAP1*[K9R,K16R] or P_{ADH1}-*GAP1*[K9R,K16R,A297V]. The mean (±SEM; n = 3) initial velocity of uptake was measured as a function of [14C]-glycine concentration. Fits to the Michaelis–Menten equation revealed similar K_m values: K_m = 20.0 ± 5.3 μM for Gap1p[K9R,K16R] and K_m = 12.7 ± 1.1 μM for Gap1p[K9R,K15R,A297V]. (C and D) Similar kinetic parameters for citrulline inhibition of [14C]-glycine uptake were determined for Gap1p[K9R,K16R] and Gap1p[K9R,K15R,A297V]. Initial velocity of uptake was measured for 4 μM [14C]-glycine in the presence of various concentrations of unlabeled citrulline. Fits to a four-parameter sigmoidal equation gave similar IC50 values: IC50 = 30.9 μM for Gap1p[K9R,K16R] and IC50 = 27.0 μM for Gap1p[K9R,K16R,A297V].

ability of amino acids to inhibit recycling of Gap1p from the MVE to the plasma membrane (Rubio-Texeira and Kaiser, 2006). To assess the effects of Gap1p mutations on the response to amino acids, we designed a redistribution assay to measure the rate of traffic of Gap1p from the MVE to the plasma membrane. The idea was to accumulate Gap1p in the MVE by expressing Gap1p in the presence of a large excess of CAS and then to shut off Gap1p synthesis for a period of time sufficient to clear newly synthesized Gap1p from the endoplasmic reticulum (ER) and Golgi compartments and then to follow the extent of redistribution of Gap1p from the MVE to the plasma membrane after removal of amino acids. An appropriately regulated form of Gap1p was constructed by placing *GAP1* under control of the *GAL10* promoter (P_{GAL10}-*GAP1*). Synthesis of P_{GAL10}-*GAP1* was induced on galactose medium supplemented with CAS. Transcription of Gap1p was stopped by incubation of cells in glucose medium with CAS for 1 h, a time sufficient for any newly synthesized Gap1p to transit the early compartments of the secretory pathway and reach the MVE. At this time, CAS was removed, and cells were placed into glucose medium with no amino acids (SD) or

with basic amino acids (SD + BAM). The redistribution assay was performed in a *car1Δ* strain, which lacks arginase, thus inhibiting conversion of arginine to glutamate and other amino acids (Sumrada and Cooper, 1982). To determine a maximum level of Gap1p reactivation after CAS removal, we followed the increase in glycine uptake over the 30 min after removal of amino acids (SD) and found that activity increased approximately 10-fold. Cells shifted into SD with BAM did not increase significantly, showing that BAM was sufficient to prevent wild-type Gap1p from redistributing to the plasma membrane (Figure 3A). In contrast to wild type, Gap1p[A297V] showed efficient redistribution to the plasma membrane in either SD or SD + BAM (Figure 3B). This crucial result showed that Gap1p[A297V], which has a specific defect in the transport of basic amino acids, also fails to be regulated by basic amino acids at the stage of amino acid–regulated sorting in the MVE.

As a control, we asked whether disruption of post-Golgi secretory vesicle–trafficking machinery could disrupt the redistribution of Gap-1p[A297V]. Previously we showed that redistribution of Gap1p observed in cells shifted from glutamate to urea as a nitrogen source requires
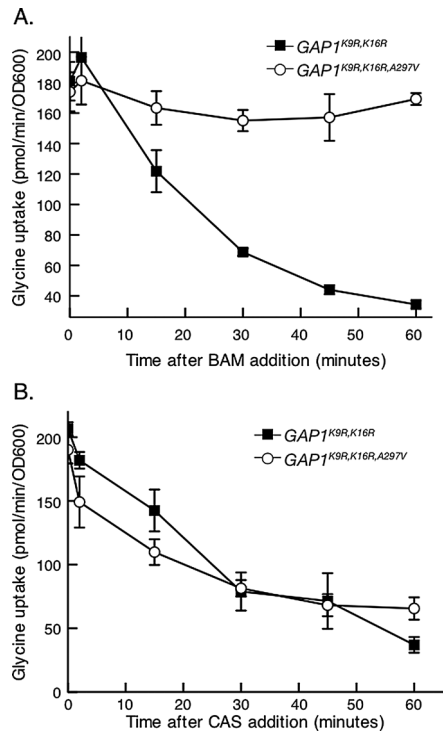
FIGURE 2: Inactivation of Gap1p at the plasma membrane requires transport of amino acid substrates. A *gap1Δ* strain (CKY482) expressing either *GAP1*[K9R,K16R] (pAR77) or *GAP1*[K9R,K16R,A297V] (pNC9) was cultured to exponential phase before addition of (A) BAM mix or (B) CAS mix. The mean (±SEM; n = 3) initial velocity of [14C]-glycine showed that Gap1p[K9R,K16R,A297V] is inactivated by CAS but not by BAM.

the exocyst complex and is blocked in temperature-sensitive mutants such as *sec6–4* (Roberg *et al.*, 1997). We anticipated that the redistribution of active Gap1p[A297V] to the plasma membrane in the presence of BAM would require vesicle trafficking and thus should be blocked in *sec6–4* at the restrictive temperature. Strains expressing Gap1p or Gap1p[A297V] were cultured in duplicate as described earlier in text, and recycling was measured at both the permissive temperature of 24°C and the restrictive temperature of 36°C. Prior to removal of CAS from the glucose medium, one culture of each strain was shifted to 36°C for 10 min, and then filtered into prewarmed SD or SD + BAM at 36°C. The control performed on Gap1p-expressing cells confirmed previous results; only cells at 24°C in SD showed reactivation (Figure 3C). Gap1p[A297V] reactivated in both SD and SD + BAM at 24°C, as observed in Figure 3B. Gap1p[A297V] was not reactivated in SD or SD + BAM at 36°C, however (Figure 3D). By comparison, Gap1p[K9R,K16R], which is constitutively present at the plasma membrane but reversibly inactivated by amino acids, increases in activity to 80% of maximum within 30 min of amino acid washout (Figure 3E). Thus we conclude that Gap1p redistributes from the MVE to the plasma membrane and that this recycling relies on the same machinery required for vesicular trafficking between the *trans*-Golgi and the plasma membrane.

To visualize the redistribution of Gap1p, we localized green fluorescent protein (GFP)-tagged Gap1p by fluorescence microscopy during the redistribution assay (Figure 4A). Prior to removal of CAS, both Gap1p-GFP and Gap1p[A297V]-GFP were primarily located in the vacuole as well as associated organelles (probably corresponding to the MVE). After removal of CAS, cells were cultured for 30 min before imaging. When transferred into medium that did not contain amino acids (SD), both Gap1p-GFP and Gap1p[A297V]-GFP were ob-
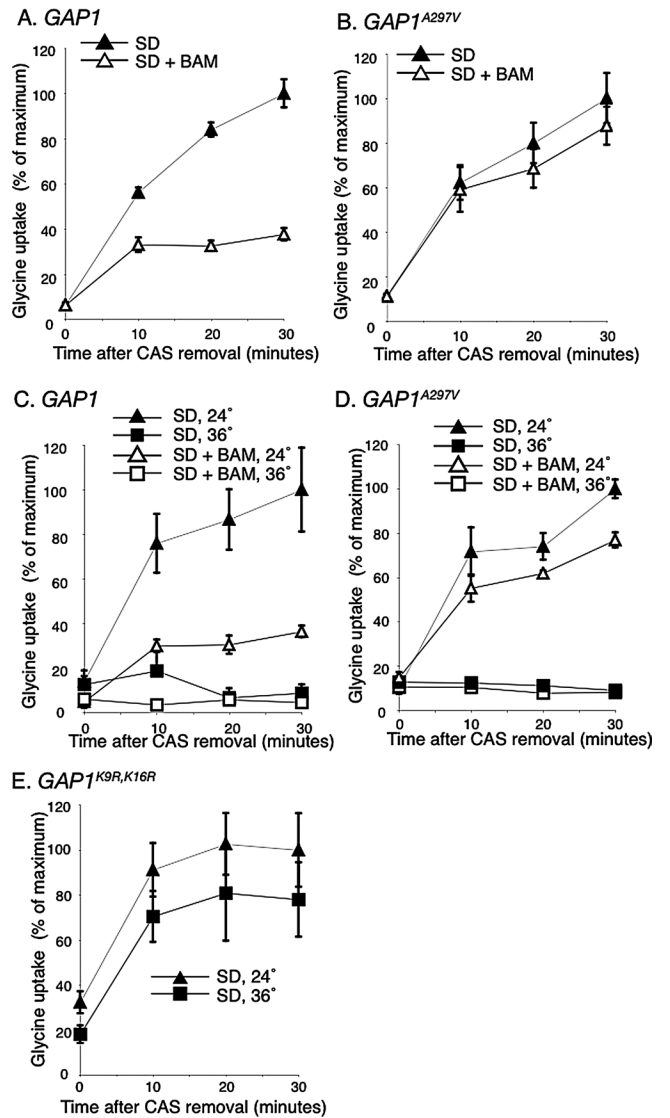
FIGURE 3: Recycling of Gap1p[A297V] to the plasma membrane is not blocked by basic amino acids. Gap1p expressed from the *GAL10* promoter in *gap1Δ car1Δ* cells was accumulated in the MVE during growth on SGal medium + CAS. After shutoff of new Gap1p expression with glucose and removal of CAS, recycling of preexisting Gap1p to the plasma membrane was measured by initial rate of [14C]-glycine uptake (±SEM; n = 5). (A) Wild-type Gap1p was recycled efficiently in the absence of CAS, but was blocked in the presence of BAM, whereas (B) Gap1p[A297V] was recycled efficiently in the presence of BAM. (C–E) The redistribution assay was performed in a *gap1Δ car1Δ sec6–4* strain expressing (C) P[GAL10]-*GAP1* (pNC26), (D) P[GAL10]-*GAP1*[A297V] (pNC27), or (E) P[GAL10]-*GAP1*[K9R,K16R] (pNC69). Where indicated, the temperature-sensitive *sec6–4* defect was imposed by shifting cells to 36°C for 10 min while in SD + CAS before removal of CAS and transfer into SD or SD+BAM medium prewarmed to 36°C. The mean initial rate of [14C]-glycine uptake (±SEM; n = 5) is shown.

served at the plasma membrane, although an appreciable amount was associated with the vacuole, probably corresponding to the pool of Gap1p already in the vacuole or irreversibly committed to transport to the vacuole at the time of amino acid removal. When transferred to SD + BAM, Gap1p-GFP did not redistribute to the plasma membrane, but Gap1p[A297V]-GFP did, to approximately the same extent as in amino acid–free medium. These localization studies confirm the results of the activity assays—that Gap1p[A297V] does
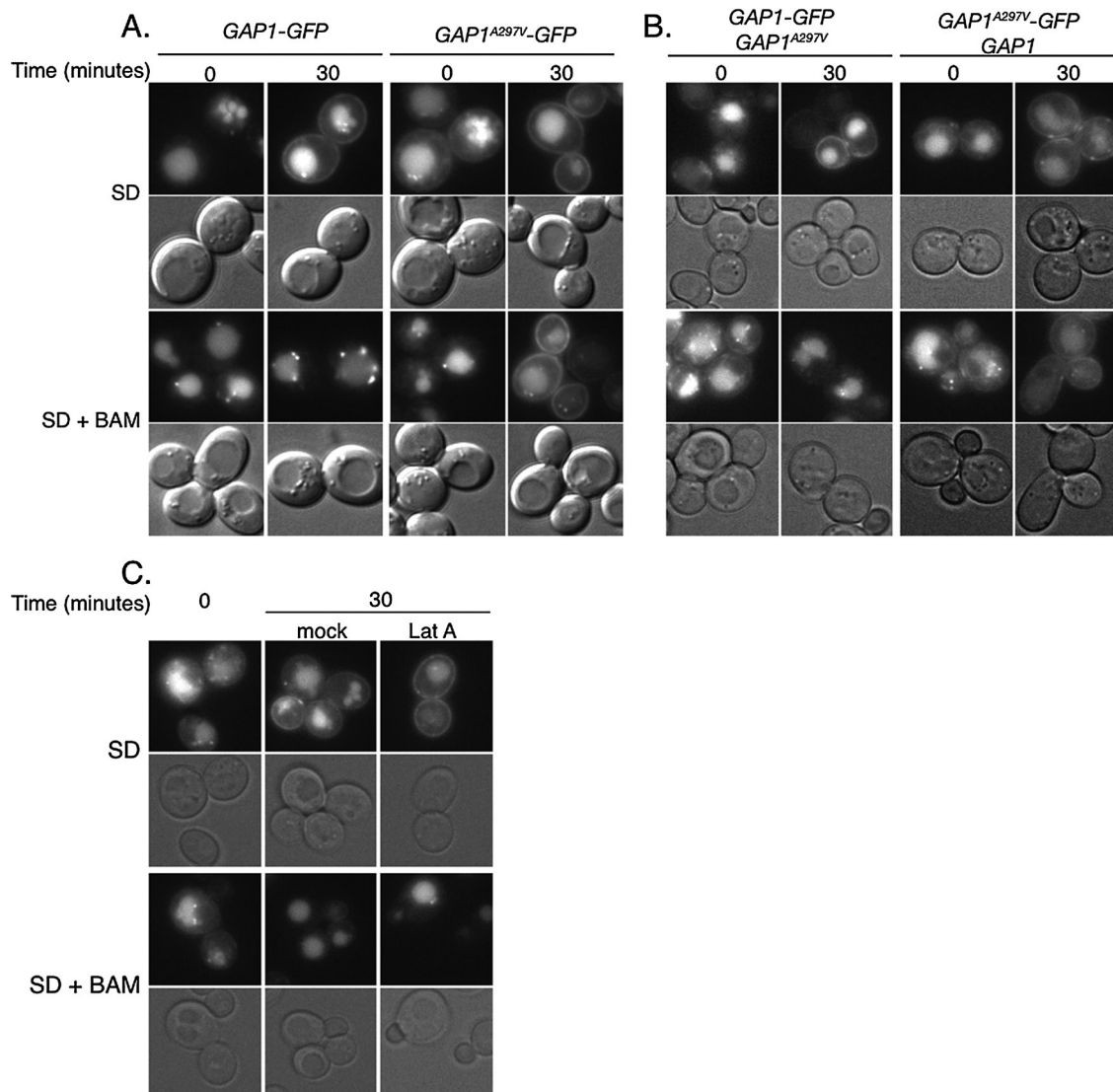
FIGURE 4: Redistribution of Gap1p^{A297V} from the MVE to the plasma membrane in the presence of basic amino acids. (A) *gap1Δ car1Δ* cells expressing P_{GAL10}-*GAP1-GFP* (pNC29) or P_{GAL10}-*GAP1^{A297V}-GFP* (pNC30) were cultured to early exponential phase in SGal medium + CAS before glucose shutoff and CAS removal. (B) *gap1Δ car1Δ* cells expressing P_{GAL10}-*GAP1-GFP* with P_{GAL1}-*GAP1^{A297V}* (pNC119) or P_{GAL10}-*GAP1^{A297V}-GFP* with P_{GAL1}-*GAP1* (pNC120) were cultured as in (A). In (C), *gap1Δ car1Δ* cells expressing P_{GAL10}-*GAP1-GFP* with P_{GAL1}-*GAP1^{A297V}* were treated with ethanol (mock) or 40 μM latrunculin A (Lat A) immediately after CAS removal. In all panels, samples were collected immediately before and 30 min after CAS removal. Gap1p-GFP was imaged by fluorescence microscopy.

not respond to the presence of basic amino acids in redistributing from the MVE to the plasma membrane.

We were concerned about the possibility that the diminished response of Gap1p^{A297V} to basic amino acids could be due to an indirect effect on intracellular amino acid pools resulting from a decreased capacity of Gap1p^{A297V} mutants to take up basic amino acids. To control for this possibility, we assayed accumulation of radiolabeled basic amino acids over the 30 min after CAS removal and found the total amino acid uptake for the Gap1p^{A297V} mutant is similar as for wild type, 17.2 and 20.1 nmol/OD$_{600}$, respectively (unpublished data). This equivalence of Gap1p mutant and wild type for basic amino acid uptake can be explained by the presence of *CAN1* and *LYP1* permeases that provide robust transport of arginine and lysine independently of Gap1p. Moreover, the contribution of wild-type Gap1p to amino acid uptake should be negligible because

both wild type and Gap1p^{A297V} mutant strains have little Gap1p permease activity after growth on CAS.

To show that the insensitivity of Gap1p^{A297V} mutant to sorting by basic amino acids is due to an intrinsic property of the mutant protein and not to some unanticipated effect of the mutant on cellular amino acid pools, we performed a *cis/trans* test, in which redistribution of GFP-tagged Gap1p or Gap1p^{A297V} was followed in heterozygotes also expressing untagged Gap1p^{A297V} or Gap1p, respectively. We observed that Gap1p-GFP did not reappear at the plasma membrane in SD + BAM even in cells expressing Gap1p^{A297V}, whereas Gap1p^{A297V}-GFP was recycled to the plasma membrane in the presence of SD + BAM even in cells also expressing wild-type Gap1p (Figure 4B). Formally these results show that the behavior of the Ala-297 to Val mutant, which is to allow trafficking to the plasma membrane even in the presence of BAM, acts in *cis* but not in *trans*.

This result shows that the mutation exerts its effect on the mutated Gap1p protein and not on the physiology of the whole cell.

Finally, we wanted to verify that wild-type Gap1p-GFP is located in internal compartments when grown in SD + BAM because of a block in recycling from the MVE to the plasma membrane and not because of an increased rate of endocytosis from the cell surface. To do this, we performed the redistribution assay as before, but treated the cells with the actin-depolymerizing drug and endocytosis inhibitor latrunculin A at the time of CAS removal to trap any Gap1p-GFP that had reached the cell surface. In both mock-treated and latrunculin-treated cells grown in SD + BAM, we observed the majority of Gap1p in internal compartments (Figure 4C), indicating that, during our redistribution assay, wild-type Gap1p does not reach the cell surface in SD + BAM medium. Therefore the localization of Gap1p in amino acids is caused by an inability to recycle from the MVE.

A catalytically inactive mutant displays reduced sensitivity to amino acid sorting

To extend the results with the substrate specificity mutant Gap1p^{A297V}, we wished to identify a catalytically inactive mutant of Gap1p that could not transport any amino acids with the expectation that such a mutant may not be regulated by any amino acids. The aim was to identify a Gap1p mutant that was specifically defective for amino acid transport but that could fold normally as judged by the ability of the mutant protein to pass the ER quality control checkpoint and be trafficked to the late secretory pathway. To find rare transport-defective mutants that were also properly folded, we took a targeted mutagenesis approach based on sequence similarity of Gap1p to prokaryotic transporter proteins for which structural information was available. A common feature of these structures is a short, unwound section in both TMD1 and TMD6. Substrate-bound forms of LeuT (Yamashita et al., 2005; Singh et al., 2008) and AdiC (Gao et al., 2010) show these regions as part of the amino acid binding site. In AdiC, Gly-25—Ser-26-Gly-27 makes up the unwound section of TMD1, and initial characterizations of AdiC showed that a Ser-26 to Lys substitution blocked antiport activity (Gao et al., 2009). This GSG motif in AdiC aligns with a conserved GTG motif in five amino acid transporters of S. cerevisiae, including Gap1p (Gly-105-Thr-106-Gly-107).

To determine whether this GTG motif in Gap1p serves a function similar to that of the GSG motif in AdiC, we generated the analogous mutation in Gap1p, Thr-106 to Lys. We tested amino acid uptake abilities of Gap1p^{T106K} and found that it was unable to import any amino acid we tested (Figure 5A), supporting the hypothesis that the GTG motif of Gap1p is involved in amino acid binding. Importantly, localization of Gap1p^{T106K}-GFP revealed that the protein was expressed and localized to the plasma membrane normally. For comparison, we show a typical randomly generated mutant, Gap1p^{T21S,C397R}-GFP, which is also inactive for uptake but is primarily located in the ER presumably because of a folding defect (Figure 5B). We tested a range of citrulline and glycine concentrations from 4 µM up to 1 mM to determine whether the loss of amino acid uptake ability of Gap1p^{T106K} was due to an increase in K_m, but we did not observe uptake of either citrulline or glycine even at the highest substrate concentrations (unpublished data). We cannot, however, rule out the possibility that Gap1p^{T106K} may have K_m for transport of some amino acids in the millimolar range.

Next we tested how sorting of Gap1p^{T106K} to the plasma membrane would respond to a complex mixture of amino acids. We expressed P_{ADH1}-GAP1-GFP or P_{ADH1}-GAP1^{T106K}-GFP in a wild-type strain cultured in SD medium. CAS was then added to half of each culture at a final concentration of 0.025% (corresponding to a total amino acid concentration of 1–2 mM), an amount in approximately
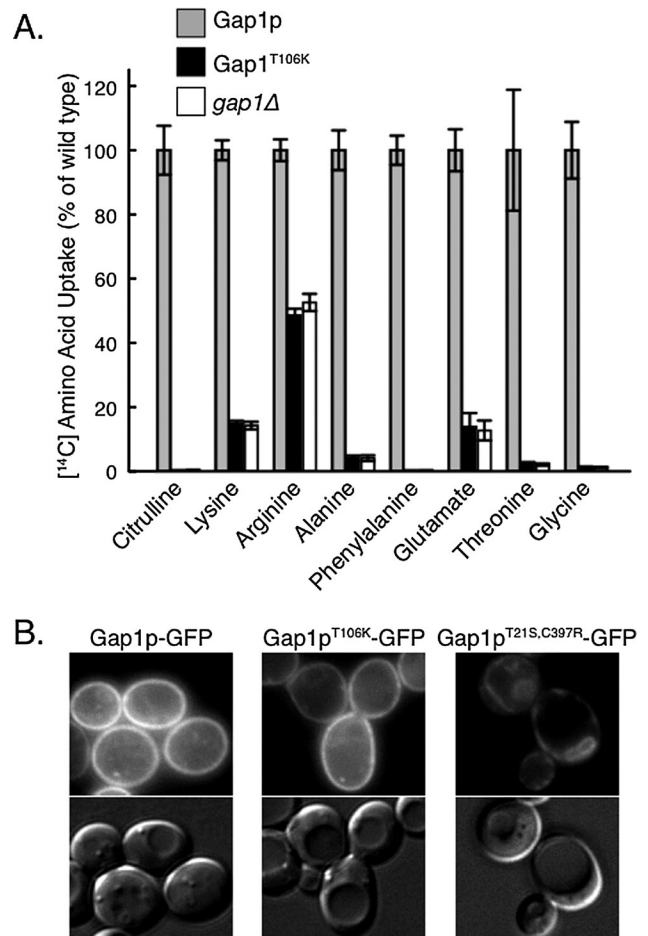
FIGURE 5: The Gap1^{T106K} mutant has a general defect in amino acid transport. (A) *ADH1*-promoted wild-type *GAP1* (pEC221), Gap1^{T106K} (pNC74), or empty vector (pRS316) were expressed in a *gap1Δ bul1Δ bul2Δ* (CKY701) strain grown in SD medium. Initial rate of uptake was determined for the [^{14}C]-labeled amino acids indicated. Mean uptake rates (n = 3) were normalized to the wild-type rate for each amino acid. (B) P_{ADH1}-*GAP1-GFP* (pAR13), P_{ADH1}-*GAP1^{T106K}-GFP* (pNC84), or P_{ADH1}-*GAP1^{T21S,C397R}* (pNC113) was expressed in CKY701 cells grown in SD medium. Gap1p-GFP was imaged by fluorescence microscopy.

10-fold excess of the minimum concentration needed to signal direct sorting of Gap1p to the vacuole (Risinger et al., 2006). As expected, wild-type Gap1p-GFP was located primarily in internal compartments, including the vacuole, after 3 h of growth in SD + 0.025% CAS, but Gap1p^{T106K}-GFP was observed both at the plasma membrane and in the vacuole (Figure 6A). Because we were interested in assessing direct sorting to the vacuole independently of endocytosis, we used an *end3Δ* mutant to block endocytosis of Gap1p from the plasma membrane (Tang et al., 1997). In an *end3Δ* mutant, any Gap1p present in the vacuole must have reached that location by direct sorting via the *trans*-Golgi and MVE, because the endocytic pathway from the plasma membrane to the vacuole is blocked. Wild-type Gap1p-GFP was located primarily at the plasma membrane when grown in SD, but was located primarily in the vacuole after 3 h of growth in SD + 0.025% CAS. A small amount of Gap1p-GFP was seen at the plasma membrane in some cells, presumably corresponding to Gap1p-GFP that was localized to the plasma membrane before the addition of CAS and was trapped there because of *end3Δ*. In contrast, Gap1p^{T106K} was located primarily in the plasma membrane when cells were grown in either SD or
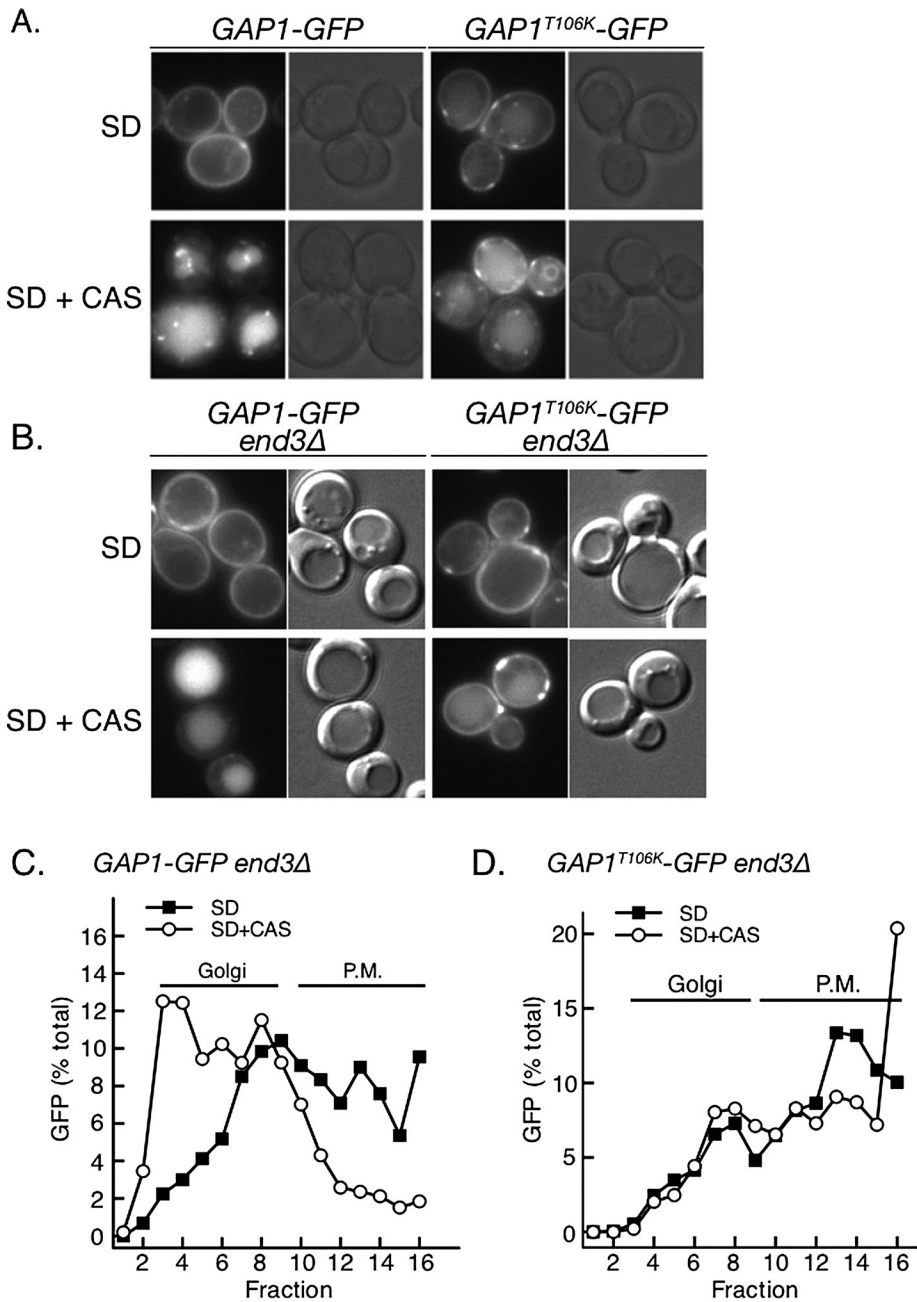
FIGURE 6: Gap1p^T106K-GFP is sorted to the vacuole even in the presence of amino acids. P_ADH1-GAP1-GFP (pAR13) or P_ADH1-GAP1^T106K-GFP (pNC84) was expressed in (A) gap1Δ or (B–D) gap1Δ end3Δ cells and grown in SD. Where indicated, 0.025% CAS was added for 3 h. (A and B) Gap1p-GFP was imaged by fluorescence microscopy. (C and D) Quantitation of cellular distribution of Gap1p-GFP and Gap1p^T106K-GFP measured by cell fractionation. Lysates were prepared and fractionated over a continuous 20–60% sucrose gradient with 10 mM EDTA. Proteins were separated by SDS–PAGE and immunoblotted with anti-GFP or or anti-Pma1p. Golgi fractions were identified by GDPase activity. Gel images and GDPase activity graphs are shown in Supplemental Figure 1.

membrane from Golgi and MVE compartments. Membranes from end3Δ cells expressing P_ADH1-GAP1-GFP or P_ADH1-GAP1^T106K-GFP grown in either SD or SD + 0.025% CAS were separated over a continuous 20–60% sucrose gradient in the presence of EDTA. Under these conditions, the plasma membrane, identified by the marker Pma1p, fractionates at a considerably higher density than do intracellular membranes, including the Golgi (identified by GDPase activity), MVE, and ER (Supplemental Figure S1). After growth in SD, Gap1p-GFP was present both in the plasma membrane and in internal fractions in approximately equal amounts. After 3 h of growth in SD + 0.025% CAS, however, the majority of Gap1p-GFP fractionated in internal membranes, with only a small amount still seen at the plasma membrane (Figure 6C and Supplemental Figure S1A). The pool of Gap1p at the plasma membrane in CAS probably corresponds to Gap1p that was sorted to the plasma membrane before the addition of CAS and was prevented from reaching the vacuole by endocytosis due to the end3Δ mutation. Gap1p^T106K-GFP is primarily observed at the plasma membrane both in SD and SD with amino acids, with more than 70% cofractionating with Pma1p (Figure 6D and Supplemental Figure S1B).

We considered the possibility that Gap1p^T106K is inefficiently sorted to the vacuole in CAS because of lower levels of amino acid import than observed in wild-type cells. Therefore we also performed fluorescence microscopy on Gap1p^T106K-GFP in an end3Δ strain also expressing wild-type Gap1p (expressed constitutively from P_ADH1-GAP1 promoter fusion). Even in the presence of wild-type Gap1p, the majority of Gap1p^T106K-GFP was located at the plasma membrane (Supplemental Figure S2). Taken together, these fluorescence microscopy and membrane fractionation experiments show that the catalytically inactive mutant Gap1p^T106K displays a reduced sensitivity to the amino acid signal for sorting to the vacuole.

DISCUSSION
Through the use of mutants that alter the substrate specificity or activity of Gap1p, we have shown that a given amino acid must be a transport substrate for Gap1p to

SD + 0.025% CAS, to a greater extent than was observed in wild-type cells (Figure 6B). Therefore it appears that the vacuolar population of Gap1p^T106K in wild-type cells is primarily due to endocytosis from the plasma membrane and not direct sorting from the trans-Golgi.

Because Gap1p^T106K is catalytically inactive we could not use activity assays to confirm the localization of this protein to the plasma membrane. Instead we used density gradients to fractionate plasma

create a signal that inhibits trafficking of Gap1p from the MVE to the plasma membrane. The Gap1p^A297V mutant does not transport citrulline and arginine nor does it respond to these amino acids for regulated intracellular sorting. Nevertheless, citrulline and arginine can competitively inhibit glycine uptake through Gap1p^A297V, showing that, although the Ala-297 to Val substitution blocks the full translocation of basic amino acids, the ability of citrulline and arginine to compete with glycine transport suggests that basic amino

acids bind to the active site of the transporter with normal affinity. Therefore binding of Gap1p to its substrate is not sufficient to signal sorting. Rather, a transport cycle is required. This dependence on transport activity would distinguish the mode of regulated sorting of Gap1p from the many examples of plasma membrane proteins that are down-regulated in response to the binding of their substrates, such as the manganese transporter Smf1p (Liu and Culotta, 1999; Jensen *et al.*, 2009) and the uracil permease Fur4p (Seron *et al.*, 1999; Blondel *et al.*, 2004).

We were not able to perform similar tests of the effect of the Gap1p^{T106K} mutation on the transport cycle as the complete lack of amino acid transport in these mutants prevented measurement of amino acid binding by competition experiments. Existing structural data offer clues to the defect of Gap1p^{T106K}. In the recently solved crystal structure of AdiC, Ser-26 is shown to form a hydrogen bond with the α-carboxylate of its substrate arginine (Gao *et al.*, 2010). As Ser-26 of AdiC corresponds to Thr-106 of Gap1p, it is likely that the Thr-106 to Lys substitution disrupts amino acid binding, presumably preventing it from completing a transport cycle. Thus it appears that substrate transport and regulation of intracellular trafficking are therefore tightly coupled such that, in the absence of amino acid translocation, Gap1p does not sense the presence of amino acids and is trafficked to the vacuole even when amino acids are abundant. We could detect a small amount of Gap1p^{T106K}-GFP in the vacuole in cells grown in CAS indicating that Gap1p^{T106K} does retain some capacity to respond to intracellular amino acid abundance. At this stage it is not possible to ascertain whether Gap1p^{T106K} has some residual capacity to transport amino acids (with a high K_m) or whether there are secondary mechanisms for trafficking regulation that act independently of the transport cycle.

The alternate access model for APC transporter function depicted in Figure 7 (Jardetzky, 1966) provides a useful scheme for thinking about how substrate transport and trafficking fate might be coupled. As Gap1p alternates between extracellular and cytoplasm-facing states at the plasma membrane to facilitate transport of amino acids into the cell, it may similarly alternate between exoplasm- and cytoplasm-facing states on the MVE membrane to signal for either recycling to the plasma membrane or vacuolar sorting, respectively. Although the kinetics of the transport cycle of Gap1p have not been determined, if isomerization of empty Gap1p from the cytoplasmic state to the exoplasmic state (CF to EF; step 4) is significantly slower than substrate translocation (EB to CB; step 2), an increase in amino acids on the exoplasmic face should lead to an abundance of the cytoplasmically oriented state (CF or CB) relative to the exoplasmically oriented state (EF or EB). This idea, combined with the observation that a mutant unable to perform step 2 is efficiently recycled from the MVE, suggests the following model: When Gap1p assumes the cytoplasmically oriented state, it is blocked from recycling, leading to its internalization into intralumenal vesicles (ILVs) and delivery to the vacuole. Conversely, when amino acids are scarce, the majority of Gap1p present on the MVE membrane would be in the exoplasmically oriented state, which would be competent for recycling and sorting to the plasma membrane.
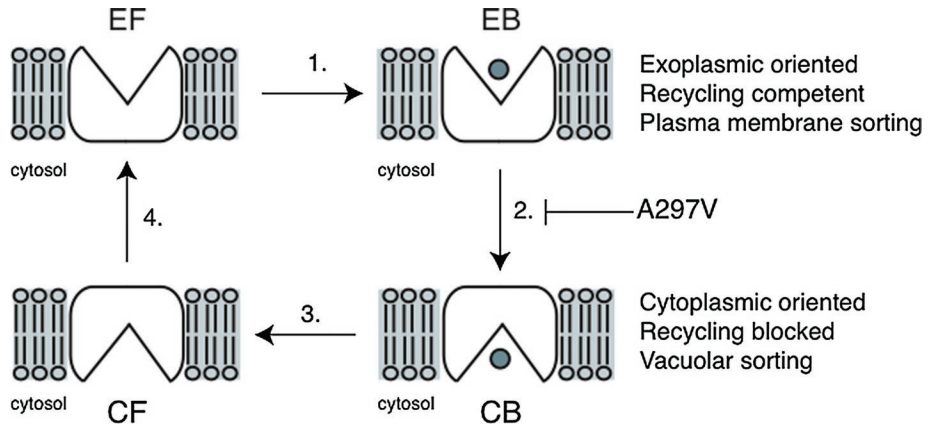
FIGURE 7: The alternate access model for substrate transport showing how the conformational state may switch in response to amino abundance. During the transport cycle, Gap1p assumes four different states: exoplasmically oriented free (EF), exoplasmically oriented bound (EB), cytoplasmically oriented bound (CB), and cytoplasmically oriented free (CF). In state EF or EB, Gap1p would be competent to recycle from the MVE to the plasma membrane. In CF or CB, Gap1p would be prevented from recycling and would enter ILVs destined for the vacuole. The Ala-297 to Val mutation in Gap1p prevents the transition from EB to CB (step 2) for basic amino acids, preventing Gap1p from switching to cytoplasmically oriented, thus preventing vacuolar trafficking of Gap1p in response to basic amino acids.

We can imagine two ways in which the conformational state of Gap1p could affect the propensity to recycle from the MVE membrane. The first is that the cytoplasmically oriented state could more efficiently interact with the endosomal sorting complexes required for transport (ESCRT) machinery, increasing the efficiency of ILV formation. Because internalization into ILV requires the recognition of ubiquitinated cargo (Urbanowski and Piper, 2001), the cytoplasmic state could make the ubiquitinated N terminus of Gap1p more accessible to ESCRT. Gap1p in the EF or EB conformations would therefore be left on the MVE membrane until it is recycled to the Golgi by a passive process. Alternatively, the exoplasmically oriented state could more efficiently interact with the as yet undefined components necessary for recycling, leaving the cytoplasmically oriented state on the MVE membrane to be internalized into ILV by ESCRT. Although we did not observe a noticeable defect in ubiquitination of Gap1p^{A297V} or Gap1p^{T106K} in the presence of BAM or CAS, respectively (Supplemental Figure S3), we cannot rule out the former possibility, as ubiquitin recognition by ESCRT could also be affected by deubiquitination of Gap1p on the MVE membrane.

The model we propose bears some similarity to that of dual-function amino acid transporter/receptor, or "transceptor" proteins (Hundal and Taylor, 2009). The best understood transceptor is Ssy1p, the transporter-like amino acid sensor component of the SPS complex. Although Ssy1p resembles APC transporters, it has no detectable amino acid transport activity. Rather, signaling of amino acids such as leucine through Ssy1p is based on amino acid binding to the extracellular (exoplasmic) portion of the protein, which is thought to induce a conformational change that activates the SPS sensing response, leading to induction of permease gene expression. Because Ssy1p cannot shift from EB to CB (Figure 7, step 2), an increase in extracellular amino acids is thought to drive Ssy1p into an exoplasmically oriented conformation by mass action. This model is supported by experiments in which overproduction of intracellular leucine inhibits the response of Ssy1p to extracellular leucine, suggesting that the intracellular leucine can drive Ssy1p in a cytoplasmically oriented, nonsignaling conformation (Wu *et al.*, 2006; Poulsen *et al.*, 2008). Gap1p has also been proposed to function similarly as

a transceptor at the plasma membrane to activate PKA signaling. Because PKA pathway activation requires substrate binding by Gap1p, but not the completion of a transport cycle, Gap1p is thought to assume a unique signaling conformation distinct from the four transport cycle conformations (Donaton et al., 2003; Van Zeebroeck et al., 2009).

We propose that the examples of transceptor signaling, as typified by Ssy1p, and transport cycle–coupled signaling, as typified by the sorting of Gap1p shown here, represent two fundamentally different mechanisms by which a transporter-like protein can signal by switching its conformational state in response to a substrate concentration gradient. In the case of Ssy1p, which cannot execute an amino acid translocation step, a high concentration of amino acids on the exoplasmic side of the membrane is thought to drive Ssy1p into an exoplasmically oriented conformation, which signals amino acid abundance. In contrast, as we have shown here, intracellular sorting of Gap1p requires an amino acid translocation step to respond to the amino acid signal. It is therefore likely that Gap1p is driven into a cytoplasmically oriented conformation, which is the signal for amino acid abundance. For Ssy1p the conformational switch activates a signal transduction pathway, whereas a conformational switch in Gap1p regulates the intracellular sorting of Gap1p in the MVE. For both signaling mechanisms, it is of great interest to understand the nature of the different conformational states and how these states are recognized by either signaling or protein-sorting machinery.

MATERIALS AND METHODS
Strains, plasmids, and media
All of the yeast strains used in this study (Table 1) were constructed in the S288C genetic background. Wild-type S288C strains exhibit relatively high Gap1p activity in ammonia medium, in contrast to strains in the Σ1278b genetic background, which exhibit low Gap1p activity when grown on ammonia (Stanbrough and Magasanik, 1995). Deletions of CAR1 and END3 were made by one-step gene replacement in CKY482. Disruption of CAR1 was verified by loss of ability to use arginine as a sole nitrogen source. Disruption of END3 was verified by PCR.

Plasmids used in this study are listed in Table 2. Plasmid pNC26 was constructed by amplifying the GAP1 open reading frame with an adjoining 580 bp of 3' sequence using oligos OES43 and OES44. The resulting fragment was digested with EcoRV and XhoI and ligated into pCD43 (Shaywitz et al., 1995), which was digested with EcoRI, blunted with Mung Bean nuclease, and digested again with XhoI. Plasmids containing GAP1^{T106K} and GAP1^{T106K}-GFP were created using the QuikChange kit (Stratagene, La Jolla, CA). Other mutations were introduced into the plasmid-borne GAP1 gene by subcloning mutations from existing plasmids.

Strains were grown at 24°C unless otherwise noted. Minimal ammonia medium (SD) is composed of Difco (Detroit, MI) yeast nitrogen base without amino acids or ammonium sulfate (YNB), 2% glucose, and 0.5% ammonium sulfate (adjusted to pH 4.0 with HCl). Nitrogen-free medium is SD medium without ammonium sulfate. Galactose medium (SGal) is composed of YNB, 2% raffinose, 0.25% galactose, and 0.5% ammonium sulfate (adjusted to pH 4.0 with HCl). CAS (Difco) were added from a 10% stock (pH 4) to SD or SGal at a final concentration of 0.025% or 0.25%. BAM is composed of arginine, citrulline, and lysine (Sigma, St. Louis, MO) diluted from a stock solution of 100 mM each (pH 4).

For measurement of Gap1p recycling, strains expressing P_{GAL10}-GAP1 or P_{GAL10}-GAP1-GFP were cultured ~16 h in SGal to induce Gap1p expression. CAS (0.25%) were added for 1 h to sequester Gap1p in the MVE. Cells were then filtered and suspended in SD

Strain	Genotype	Source
CKY482	MATα leu2–3 ura3–52 gap1::LEU2	Kaiser strain collection
CKY701	MATα leu2–3 ura3–52 gap1::LEU2 bul1::kanMX6 bul2::kanMX6	Kaiser strain collection
CKY703	MATa leu2–3 ura3–52 his3 gap1::LEU2	Kaiser strain collection
CKY1025	MATa leu2–3 ura3–52 gap1::LEU2 can1	Kaiser strain collection
CKY1080	MATa leu2 ura3–52 gap1::LEU2 car1::kanMX6 GAL2	This study
CKY1081	MATa ura3–52 gap1::LEU2 car1::kanMX6 sec6–4 GAL2	This study
CKY1082	MATα ura3–52 leu2 gap1::LEU2 end3::kanMX6	This study
CKY1085	MATa ura3–52 leu2,3 his3 gap1::LEU2 car1::KanMX	This study

TABLE 1: Strains

Name	Description	Markers	Source
pAR1	P_{ADH1}-HA-GAP1^{K9R,K16R}	CEN, URA3	Risinger et al. (2006)
pAR13	P_{ADH1}-GAP1-GFP	CEN, URA3	Risinger et al. (2006)
pAR77	P_{ADH1}-GAP1^{K9R,K16R}	CEN, URA3	This study
pCK227	P_{ADH1}-HA-GAP1	CEN, URA3	Chen and Kaiser (2002)
pCK231	P_{CUP1}-UB1-c-myc	2μ, HIS3	Helliwell et al. (2001)
pEC221	P_{ADH1}-GAP1	CEN, URA3	Risinger et al. (2006)
pNC7	P_{ADH1}-GAP1^{A297V}	CEN, URA3	Risinger et al. (2006)
pNC9	P_{ADH1}-GAP1^{K9R,K16R,A297V}	CEN, URA3	This study
pNC15	P_{ADH1}-HA-GAP1^{A297V}	CEN, URA3	This study
pNC26	P_{GAL10}-GAP1	CEN, URA3	This study
pNC27	P_{GAL10}-GAP1^{A297V}	CEN, URA3	This study
pNC29	P_{GAL10}-GAP1-GFP	CEN, URA3	This study
pNC30	P_{GAL10}-GAP1^{A297V}-GFP	CEN, URA3	This study
pNC69	P_{GAL10}-GAP1^{K9R,K16R}	CEN, URA3	This study
pNC74	P_{ADH1}-GAP1^{T106K}	CEN, URA3	This study
pNC84	P_{ADH1}-GAP1^{T106K}-GFP	CEN, URA3	This study
pNC113	P_{ADH1}-GAP1^{T21S,C397R}-GFP	CEN, URA3	This study
pNC115	P_{ADH1}-HA-GAP1^{T106K}	CEN, URA3	This study
pNC119	P_{GAL10}-GAP1-GFP, P_{GAL1}-GAP1^{A297V}	CEN, URA3	This study
pNC120	P_{GAL10}-GAP1^{A297V}-GFP, P_{GAL1}-GAP1	CEN, URA3	This study

TABLE 2: Plasmids

with 0.25% CAS and cultured for 1 h to arrest P_{GAL10}-$GAP1$ transcription and allow for trafficking of all protein through the early secretory pathway. The culture was then split, filtered, washed in an equal volume of nitrogen-free medium, and resuspended in either SD or SD + BAM (1 mM each of arginine, citrulline, and lysine) and cultured for an additional 30 min.

Amino acid uptake assays

Approximately 2×10^7 cells (one OD_{600} unit) in exponential phase were washed in nitrogen-free medium by filtration on 0.45 μM nitrocellulose filters before amino acid uptake was measured as described previously (Roberg et al., 1997). [^{14}C]-labeled alanine, phenylalanine, threonine, lysine, arginine, and glutamate were used at a specific activity of 125 mCi/mmol.

For estimation of the K_m for glycine transport through Gap1p^{K9R,K16R}, uptake was measured for [^{14}C]-glycine concentrations ranging from 1 to 80 μM at a specific activity of approximately 10 μCi/μmol. Inhibition of glycine transport by citrulline was measured by suspending cells in nitrogen-free medium supplemented with citrulline at concentrations ranging from 10 nM to 1 mM. K_m and IC_{50} values were calculated using BioDataFit (Chang Biosciences, Castro Valley, CA). K_I values were calculated by relating K_m and IC_{50} values (Cheng and Prusoff, 1973).

Fluorescence microscopy

For latrunculin A treatment, 1 ml of cell culture was treated with 20 μl of ethanol (mock) or 40 μM latrunculin A at the time of transfer into SD or SD + BAM. For all strains expressing $GAP1$-GFP, cells in exponential phase were harvested, suspended in phosphate-buffered saline with 10 mM NaN$_3$, and visualized via fluorescence microscopy. Images were captured with a Nikon E800 microscope (Melville, NY) equipped with a Hamamatsu digital camera (Bridgewater, NJ) with 1×1 binning. Image analysis was performed with Improvision OpenLabs 2.0 software (Lexington, MA).

Equilibrium density centrifugation and antibodies

Yeast cellular membranes were fractionated by equilibrium density centrifugation on continuous 20–60% sucrose gradients containing EDTA or MgCl$_2$ as described previously (Kaiser et al., 2002). Golgi-containing fractions were identified by measurement of GDPase activity. Plasma membrane fractions were identified by the presence of Pma1p. Gap1p-GFP and Pma1p were detected in membrane fractions by immunoblotting and imaging with the LI-COR Odyssey Infrared Imaging System (Lincoln, NE) using the following antibodies: mouse anti-GFP (Covance, Princeton, NJ), mouse anti-Pma1 (40B7; Abcam, Cambridge, MA), and IRDye 800CW goat anti-mouse (LI-COR). Quantitation was performed using ImageJ software (Abramoff et al., 2004).

REFERENCES

Abramoff MD, Magelhaes PJ, Ram SJ (2004). Image processing with Image J. Biophotonics Int 11, 36–42.

Blondel MO, Morvan J, Dupre S, Urban-Grimal D, Haguenauer-Tsapis R, Volland C (2004). Direct sorting of the yeast uracil permease to the endosomal system is controlled by uracil binding and Rsp5p-dependent ubiquitylation. Mol Biol Cell 15, 883–895.

Chen EJ, Kaiser CA (2002). Amino acids regulate the intracellular trafficking of the general amino acid permease of Saccharomyces cerevisiae. Proc Natl Acad Sci USA 99, 14837–14842.

Chen EJ, Kaiser CA (2003). LST8 negatively regulates amino acid biosynthesis as a component of the TOR pathway. J Cell Biol 161, 333–347.

Cheng Y, Prusoff WH (1973). Relationship between the inhibition constant (K1) and the concentration of inhibitor which causes 50 per cent inhibition (I50) of an enzymatic reaction. Biochem Pharmacol 22, 3099–3108.

Didion T, Regenberg B, Jorgensen MU, Kielland-Brandt MC, Andersen HA (1998). The permease homologue Ssy1p controls the expression of amino acid and peptide transporter genes in Saccharomyces cerevisiae. Mol Microbiol 27, 643–650.

Donaton MC, Holsbeeks I, Lagatie O, Van Zeebroeck G, Crauwels M, Winderickx J, Thevelein JM (2003). The Gap1 general amino acid permease acts as an amino acid sensor for activation of protein kinase A targets in the yeast Saccharomyces cerevisiae. Mol Microbiol 50, 911–929.

Forsberg H, Gilstring CF, Zargari A, Martinez P, Ljungdahl PO (2001). The role of the yeast plasma membrane SPS nutrient sensor in the metabolic response to extracellular amino acids. Mol Microbiol 42, 215–228.

Gao X, Lu F, Zhou L, Dang S, Sun L, Li X, Wang J, Shi Y (2009). Structure and mechanism of an amino acid antiporter. Science 324, 1565–1568.

Gao X, Zhou L, Jiao X, Lu F, Yan C, Zeng X, Wang J, Shi Y (2010). Mechanism of substrate recognition and transport by an amino acid antiporter. Nature 463, 828–832.

Grenson M, Hou C, Crabeel M (1970). Multiplicity of the amino acid permeases in Saccharomyces cerevisiae. IV. Evidence for a general amino acid permease. J Bacteriol 103, 770–777.

Helliwell SB, Losko S, Kaiser CA (2001). Components of a ubiquitin ligase complex specify polyubiquitination and intracellular trafficking of the general amino acid permease. J Cell Biol 153, 649–662.

Hundal HS, Taylor PM (2009). Amino acid transceptors: gate keepers of nutrient exchange and regulators of nutrient signaling. Am J Physiol Endocrinol Metab 296, E603–E613.

Iraqui I, Vissers S, Bernard F, de Craene JO, Boles E, Urrestarazu A, Andre B (1999). Amino acid signaling in Saccharomyces cerevisiae: a permease-like sensor of external amino acids and F-Box protein Grr1p are required for transcriptional induction of the AGP1 gene, which encodes a broad-specificity amino acid permease. Mol Cell Biol 19, 989–1001.

Jack DL, Paulsen IT, Saier MH (2000). The amino acid/polyamine/organocation (APC) superfamily of transporters specific for amino acids, polyamines and organocations. Microbiol (Reading, Engl). 146, 1797–1814.

Jardetzky O (1966). Simple allosteric model for membrane pumps. Nature 211, 969–970.

Jensen LT, Carroll MC, Hall MD, Harvey CJ, Beese SE, Culotta VC (2009). Down-regulation of a manganese transporter in the face of metal toxicity. Mol Biol Cell 20, 2810–2819.

Kaiser CA, Chen EJ, Losko S (2002). Subcellular fractionation of secretory organelles. Methods Enzymol 351, 325–338.

Liu XF, Culotta VC (1999). Mutational analysis of Saccharomyces cerevisiae Smf1p, a member of the Nramp family of metal transporters. J Mol Biol 289, 885–891.

Nelissen B, Wachter R, Goffeau A (1997). Classification of all putative permeases and other membrane plurispanners of the major facilitator superfamily encoded by the complete genome of Saccharomyces cerevisiae. FEMS Microbiol Rev 21, 2113–2134.

Poulsen P, Gaber RF, Kielland-Brandt MC (2008). Hyper- and hyporesponsive mutant forms of the Saccharomyces cerevisiae Ssy1 amino acid sensor. Mol Membr Biol 25, 164–176.

Risinger AL, Cain NE, Chen EJ, Kaiser CA (2006). Activity-dependent reversible inactivation of the general amino acid permease. Mol Biol Cell 17, 4411–4419.

Roberg KJ, Rowley N, Kaiser CA (1997). Physiological regulation of membrane protein sorting late in the secretory pathway of Saccharomyces cerevisiae. J Cell Biol 137, 1469–1482.

Rubio-Texeira M, Kaiser CA (2006). Amino acids regulate retrieval of the yeast general amino acid permease from the vacuolar targeting pathway. Mol Biol Cell 17, 3031–3050.

Seron K, Blondel MO, Haguenauer-Tsapis R, Volland C (1999). Uracil-induced down-regulation of the yeast uracil permease. J Bacteriol 181, 1793–1800.

Shaywitz DA, Orci L, Ravazzola M, Swaroop A, Kaiser CA (1995). Human SEC13Rp functions in yeast and is located on transport vesicles budding from the endoplasmic reticulum. J Cell Biol 128, 769–777.

Singh SK, Piscitelli CL, Yamashita A, Gouaux E (2008). A competitive inhibitor traps LeuT in an open-to-out conformation. Science 322, 1655–1661.

Soetens O, De Craene JO, Andre B (2001). Ubiquitin is required for sorting to the vacuole of the yeast general amino acid permease, Gap1. J Biol Chem 276, 43949–43957.

Stanbrough M, Magasanik B (1995). Transcriptional and posttranslational regulation of the general amino acid permease of Saccharomyces cerevisiae. J Bacteriol 177, 94–102.

Sumrada RA, Cooper TG (1982). Isolation of the CAR1 gene from Saccharomyces cerevisiae and analysis of its expression. Mol Cell Biol 2, 1514–1523.

Tang HY, Munn A, Cai M (1997). EH domain proteins Pan1p and End3p are components of a complex that plays a dual role in organization of the cortical actin cytoskeleton and endocytosis in Saccharomyces cerevisiae. Mol Cell Biol 17, 4294–4304.

Urbanowski JL, Piper RC (2001). Ubiquitin sorts proteins into the intralumenal degradative compartment of the late-endosome/vacuole. Traffic 2, 622–630.

Van Zeebroeck G, Bonini BM, Versele M, Thevelein JM (2009). Transport and signaling via the amino acid binding site of the yeast Gap1 amino acid transceptor. Nat Chem Biol 5, 45–52.

Wu B, Ottow K, Poulsen P, Gaber RF, Albers E, Kielland-Brandt MC (2006). Competitive intra- and extracellular nutrient sensing by the transporter homologue Ssy1p. J Cell Biol 173, 327–331.

Yamashita A, Singh SK, Kawate T, Jin Y, Gouaux E (2005). Crystal structure of a bacterial homologue of Na$^+$/Cl$^-$-dependent neurotransmitter transporters. Nature 437, 215–223.